AIMS Mathematics, 10(6): 14629–14656.
DOI:10.3934/math.2025659
Received: 12 April 2025
Revised: 14 June 2025
Accepted: 18 June 2025
Published: 26 June 2025

https://www.aimspress.com/journal/Math

Research article

Complex dynamics of a discretized Rosenzweig–MacArthur prey-predator model with fear effect on prey and prey refuge

Md. Jasim Uddin[1,*], Md. Mutakabbir Khan[1], Ibraheem M. Alsulami[2] and Amer Alsulami[3]

[1] Department of Mathematics, University of Dhaka,Dhaka-1000, Dhaka, Bangladesh
[2] Mathematics Department, Faculty of Science, Umm Al-Qura University, Makkah 21955, Saudi Arabia
[3] Department of Mathematics, Turabah University College, Taif University, Taif 21944, Saudi Arabia

* **Correspondence:** Email: jasim.uddin@du.ac.bd.

Abstract: This work explores a discrete-time predator-prey system governed by a prey-dependent Rosenzweig–MacArthur response, incorporating the fear effect in prey dynamics. The study examines equilibrium properties and bifurcation mechanisms, particularly near the interior fixed point, highlighting their ecological significance. Various bifurcation types, including period-doubling and Neimark-Sacker, are identified, with precise conditions ensuring the latter's occurrence. To manage the system's intricate behavior, Ott-Grebogi-Yorke (OGY) and state feedback control are implemented. Numerical simulations reinforce theoretical findings through phase space reconstructions, Lyapunov exponent analysis, bifurcation diagrams, and local stability assessments, offering a comprehensive perspective on system transitions and control strategies.

Keywords: prey-predator model; codimension-1 bifurcations; fear-effect; refuge; chaos control
Mathematics Subject Classification: 40A05, 70K50, 92D25

1. Introduction

The intricate nature of population models has long captivated researches [1–4]. These models encompass various dynamic aspects, including population size, age structure, and numerous ecological influences. In predator-prey systems involving multiple interdependent species, external environmental factors such as seasonal fluctuations, harvesting pressure, and time delays can give rise to both chaotic dynamics and periodic oscillations [5–7]. The emergence of bifurcations and chaos in these models is often driven by density-dependent shifts from stabilizing to destabilizing regimes [8–10].

Deterministic chaos remains a central focus in ecological, mathematical, and physical sciences, particularly due to its implications for system stability and species persistence. Ecological systems

inherently possess mechanisms, such as positive feedback loops that facilitate the onset of chaotic dynamics. A seminal contribution in this domain was made by Hastings and Powell [11], who introduced a three-species food chain model demonstrating chaos under biologically plausible parameter choices. Their findings highlighted the extreme sensitivity of system trajectories to initial conditions and parameter variations, where even minor perturbations could drastically alter long-term behavior. This sensitivity underscores the ecological risks associated with chaotic regimes, as they may heighten the probability of species extinction. Consequently, investigating predator-prey interactions under the influence of key ecological drivers has garnered increasing attention from researchers seeking to understand and mitigate such complexities [12, 13].

The exploration of discrete-time systems has significantly advanced our understanding of the intricate dynamical behaviors exhibited across various disciplines. Foundational research in this domain, including studies on discretized quasiperiodic plasma perturbations [14, 15], fractional-order predator-prey models [16–18], discrete economic frameworks [19, 20], and competitive game-theoretic systems [21, 22], has been instrumental in deciphering the multifaceted nature of discrete dynamics. These pioneering contributions have shed light on diverse phenomena, ranging from the emergence of intricate oscillatory structures in plasma systems to the profound influence of fractional-order effects on ecological interactions. Furthermore, they have deepened insights into the nonlinear mechanisms governing economic fluctuations and the strategic complexity inherent in competitive systems, collectively broadening the theoretical and applied scope of discrete dynamical analysis. The study in [23, 24] examined diffusive predator-prey models by thoroughly investigating how different factors influence the system's dynamics, focusing on a comprehensive analysis of bifurcation scenarios.

The study of prey-predator dynamics in ecology and mathematical biology focuses on system persistence and stability. Prey often utilize refuges, safe zones that reduce predation risk, enhancing model realism [25–27], with several studies examining their stabilizing effects [28–31]. Predator feeding behavior also plays a crucial role; while some models assume a constant digestion rate, the Rosenzweig–MacArthur (R-M) model [32] accounts for variable consumption rates through the Holling type-II functional response, where predation initially rises with prey density but saturates due to handling constraints. Rosenzweig [33, 34] further highlighted the "paradox of enrichment", showing that increasing prey carrying capacity can destabilize ecosystems, potentially leading to species extinction, underscoring the complex interplay of ecological forces.

The fear effect, emphasizing predators' non-lethal impact on prey, is a key topic in mathematical ecology. Fear alters prey behavior, physiology, and distribution, influencing ecological dynamics. [35] examines anti-predator behavior in a Holling-type II model with prey refuge, while [36] explores fear's role in prey population growth. Building on the classical Rosenzweig–MacArthur predator-prey framework with the incorporation of fear effects, this study develops a discrete-time predator-prey model where predator dynamics are partially regulated by prey abundance [37]. A comprehensive dynamical analysis is conducted, with a particular focus on system stability and bifurcation phenomena, employing the center manifold theorem and bifurcation theory to uncover critical transitions in population dynamics. These findings provide deeper ecological insights into predator-prey interactions, highlighting the role of fear in shaping population stability and offering implications for ecosystem management. Furthermore, the study examines the onset of chaotic dynamics and investigates chaos control strategies using the OGY (Ott-Grebogi-Yorke) and state feedback control method, demonstrating potential approaches to mitigate unpredictable population fluctuations and

enhance ecological stability.

The structure of this paper is as follows: Section 2 introduces the mathematical framework of the model and its underlying formulation. In Section 3, we systematically determine the equilibrium points of the model and conduct a rigorous stability analysis. Section 4 establishes the conditions for the emergence of PD and NS bifurcations, providing a comprehensive theoretical foundation. Numerical simulations, presented in Section 5, corroborate the analytical results and illustrate key dynamical behaviors, including Neimark-Sacker bifurcations and chaotic regimes. Section 6 investigates strategies for controlling chaos within the system, and finally, Section 7 synthesizes the main conclusions, emphasizing the broader implications of the study.

2. Model formulation

The formulation of the prey-dependent Rosenzweig–MacArthur predator–prey model incorporating the fear effect is given by:

$$\begin{cases} \frac{dx}{dt} = rx\left(1 - \frac{x}{k}\right)\frac{1}{1+py} - \frac{(1-m)xy}{\beta+(1-m)x}, \\ \frac{dy}{dt} = y\left(-d + \frac{\eta(1-m)x}{\beta+(1-m)x}\right). \end{cases} \tag{2.1}$$

The initial population densities are given by $x(0) > 0$ and $y(0) > 0$, where x and y denote the prey and predator densities at any time t, respectively. The parameter r represents the intrinsic growth rate of the prey, while k defines its environmental carrying capacity. The predator's consumption of prey is governed by a prey-dependent Rosenzweig–MacArthur functional response, expressed as $\frac{(1-m)xy}{\beta+(1-m)x}$, where $m \leq 1$ accounts for the prey refuge effect. Additionally, the prey population is influenced by a fear effect, and authors in [38] used the mathematical form, modeled by the term $\frac{1}{1+py}$, with $p > 0$ quantifying the intensity of this behavioral response. From a biological standpoint, field studies suggest that the presence of fear leads to a decline in reproductive rates. All other parameters r, k, β, d, and η are assumed to be positive.

By employing the Euler scheme with a step size δ in (2.1), we obtain a discrete predator-prey system that effectively captures these dynamics with clarity and accuracy.

$$\begin{aligned} x_{n+1} &= x_n + \delta\left[rx_n\left(1 - \frac{x_n}{k}\right)\frac{1}{1+py_n} - \frac{(1-m)x_ny_n}{\beta+(1-m)x_n}\right], \\ y_{n+1} &= y_n + \delta y_n\left[-d + \frac{\eta(1-m)x_n}{\beta+(1-m)x_n}\right]. \end{aligned} \tag{2.2}$$

3. Fixed points and their stability analysis

Fixed points, often termed equilibrium states or steady states, are fundamental to the analysis of dynamical systems. These points signify conditions where the system ceases to evolve, as the equations governing its dynamics yield no change over time. The study of fixed points provides profound insights into the system's long-term behavior and has diverse applications across fields like physics, biology, engineering, and economics [36]. They are essential for understanding stability, designing effective control mechanisms, and predicting future system states [39].

3.1. Existence of fixed points

The fixed points of model (2.2) are derived by solving the following equations:

$$\begin{cases} x^* = x^* + \delta\left[rx^*\left(1-\frac{x^*}{k}\right)\frac{1}{1+py^*} - \frac{(1-m)x^*y^*}{\beta+(1-m)x^*}\right], \\ y^* = y^* + \delta y^*\left[-d + \frac{\eta(1-m)x^*}{\beta+(1-m)x^*}\right]. \end{cases}$$

Through explicit computation, the fixed points of model (2.2) are obtained as follows:

$\tilde{\xi}_0 = (0,0)$ is a trivial fixed point;

$\tilde{\xi}_1 = (k,0)$ is a semi-trivial fixed point in the absence of predator;

$\tilde{\xi}_2 = (x^*, y^*)$ is the first coexistence fixed point, where $x^* = \frac{\beta d}{(m-1)(d-\eta)}$ and $y^* = \frac{1}{2p}\left(-1 + \sqrt{1 + \frac{4rp}{1-m}(1-\frac{x^*}{k})(\beta+(1-m)x^*)}\right)$.

Lemma 1. *For the model described in Eq (2.2), the following properties hold:*

i) Regardless of the parameter values, model (2.2) always possesses a trivial fixed point $\tilde{\xi}_0 = (0,0)$ and a semi-trivial fixed point $\tilde{\xi}_1 = (k,0)$.
ii) When all positive parameters satisfy the conditions $x^* < k$ and $\eta > d$, model (2.2) has a unique coexistence fixed point given by $\tilde{\xi}_2 = (x^*, y^*)$.

3.2. Evaluating stability for fixed points

To evaluate the stability of system (2.2) at the equilibrium point $\tilde{\xi}(x,y)$, we examine the eigenvalues of the Jacobian matrix computed at this point. The local stability of $\tilde{\xi}(x,y)$ is predominantly determined by the magnitude of these eigenvalues. At this equilibrium, the Jacobian matrix is written as:

$$J(x,y) = \begin{pmatrix} \frac{\delta r(k-2x)}{kpy+k} + \frac{\beta\delta(m-1)y}{(\beta-mx+x)^2} + 1 & \delta\left(\frac{prx(x-k)}{k(py+1)^2} - \frac{x-mx}{\beta-mx+x}\right) \\ -\frac{\beta\delta\eta(m-1)y}{(\beta-mx+x)^2} & -d\delta + \frac{\delta\eta(m-1)x}{(m-1)x-\beta} + 1 \end{pmatrix}. \tag{3.1}$$

The characteristic polynomial of the Jacobian matrix (3.1) can be expressed as:

$$P(\nu) \quad = \nu^2 - \Lambda\nu + \Upsilon = 0,$$

where Λ and Υ represent the trace and determinant of $J(x,y)$, respectively.

Proposition 1. *The fixed point $\tilde{\xi}_0$ is always a saddle point.*

Proof. At the fixed point $\tilde{\xi}_0$, the Jacobian matrix is given by:

$$J(\tilde{\xi}_0) = \begin{pmatrix} \delta r + 1 & 0 \\ 0 & 1 - d\delta \end{pmatrix}.$$

The eigenvalues of $J(\tilde{\xi}_0)$ are computed as:

$$\nu_1 = 1 - d\delta, \quad \nu_2 = \delta r + 1.$$

From these eigenvalues, it is evident that $|\nu_1| < 1$, indicating stability along one direction, while $|\nu_2| > 1$, implying instability in the other direction. This confirms that $\tilde{\xi}_0$ is a saddle point. □

Proposition 2. *Let*

$$\epsilon_1 = -d, \quad \epsilon_2 = \frac{k\eta(1-m)}{k(m-1)-\beta}.$$

Then, the predator-free fixed point $\tilde{\xi}_1(k,0)$ is classified as follows:

(i) If $\epsilon_2 > \epsilon_1$, then:

(i.1) $\tilde{\xi}_1(k,0)$ is a sink if

$$0 < \delta < \min\left\{\frac{2}{r}, \frac{2}{\epsilon_2-\epsilon_1}\right\},$$

(i.2) $\tilde{\xi}_1(k,0)$ is a source if

$$\delta > \max\left\{\frac{2}{r}, \frac{2}{\epsilon_2-\epsilon_1}\right\},$$

(i.3) $\tilde{\xi}_1(k,0)$ is non-hyperbolic if

$$\delta = \frac{2}{r} \quad \text{or} \quad \delta = \frac{2}{\epsilon_2-\epsilon_1}.$$

(ii) If $\epsilon_2 < \epsilon_1$, then:

(ii.1) $\tilde{\xi}_1(k,0)$ is a source if $\delta > \frac{2}{r}$,
(ii.2) $\tilde{\xi}_1(k,0)$ is a saddle if $\delta < \frac{2}{r}$,
(ii.3) $\tilde{\xi}_1(k,0)$ is non-hyperbolic if $\delta = \frac{2}{r}$.

(iii) If $\epsilon_2 = \epsilon_1$, then $\tilde{\xi}_1(k,0)$ is non-hyperbolic for all δ.

Proof. It can be obtained that,

$$J(\tilde{\xi}_1) = \begin{pmatrix} 1-\delta r & -\frac{\delta k(m-1)}{k(m-1)-\beta} \\ 0 & -d\delta + \frac{\delta\eta k(m-1)}{k(m-1)-\beta} + 1 \end{pmatrix}.$$

The eigenvalues are $\nu_1 = 1-\delta r$ and $\nu_2 = \delta\epsilon_1 - \delta\epsilon_2 + 1$, where $\epsilon_1 = -d$ and $\epsilon_2 = \frac{k\eta(1-m)}{k(m-1)-\beta}$. From here on, the conditions for identifying sources, sinks, saddles, and non-hyperbolic fixed points can be rigorously derived and directly justified based on the properties of their eigenvalues. □

One eigenvalue of $J\left(\tilde{\xi}_1\right)$ is naturally -1, while the remaining one is not equal to ± 1 when $\delta = \frac{2}{r}$ or $\delta = \frac{2}{\epsilon_2-\epsilon_1}$. Consequently, a PD bifurcation may happen when the parameters approach the critical sets $\widehat{\Omega}^1_{\tilde{\xi}_1}$ or $\widehat{\Omega}^2_{\tilde{\xi}_1}$, respectively defined by

$$\widehat{\Omega}^1_{\tilde{\xi}_1} = \left\{(r,m,k,\beta,p,\delta,d,\eta) \in \mathbb{R}^8_+ : \delta = \frac{2}{r}, \delta \neq \frac{2}{\epsilon_2-\epsilon_1}\right\},$$

and

$$\widehat{\Omega}^2_{\tilde{\xi}_1} = \left\{(r,m,k,\beta,p,\delta,d,\eta) \in \mathbb{R}^8_+ : \delta \neq \frac{2}{r}, \delta = \frac{2}{\epsilon_2-\epsilon_1}\right\}.$$

At $\tilde{\xi}_2(x^*,y^*)$ where $y^* = \frac{1}{2p}\left(-1 + \sqrt{1 + \frac{4rp}{1-m}(1-\frac{x^*}{k})(\beta+(1-m)x^*)}\right)$, the characterizing equation can be written as follows:

$$F(\nu) := \nu^2 - (2 + \tilde{\mathcal{D}}\delta)\nu + (1 + \tilde{\mathcal{D}}\delta + \tilde{\mathcal{M}}\delta^2) = 0,$$

where

$$\tilde{\mathcal{D}} = \frac{\begin{array}{l} -(m-1)(x^*)^2\left(k(m-1)py^*(d-\eta) + dk(m-1) + \eta k - \eta km - kmr + kr - 4\beta r\right) \\ -\beta x^*\left(k(m-1)py^*(2d-\eta) + 2dk(m-1) + \eta k - \eta km - 2kmr + 2kr - 2\beta r\right) \\ +\beta k\left(y^*(\beta dp - m + 1) + \beta(d-r) + (y^*)^2(p-mp)\right) \\ +2(m-1)^2 r(x^*)^3 \end{array}}{(kpy^* + k)(\beta - mx^* + x^*)^2},$$

$$\tilde{\mathcal{M}} = \frac{\begin{array}{l} -(m-1)r(x^*)^2\Big(4\beta d + py^*(4\beta d + dk(m-1) + \eta(-3\beta + k(-m) + k)) \\ \qquad + dk(m-1) + \eta(-2\beta + k(-m) + k)\Big) \\ +\beta r x^*\left(2d(\beta + k(m-1)) + 2py^*(d(\beta + k(m-1)) - \eta k(m-1)) - \eta k(m-1)\right) \\ -\beta dk(py^* + 1)\left((m-1)p(y^*)^2 + (m-1)y^* + \beta r\right) \\ +2(m-1)^2 r(x^*)^3(d-\eta)(py^* + 1) \end{array}}{k(py^* + 1)^2(\beta - mx^* + x^*)^2}.$$

So, $F(1) = \tilde{\mathcal{M}}\delta^2 > 0$ and $F(-1) = 4 + 2\tilde{\mathcal{D}}\delta + \tilde{\mathcal{M}}\delta^2$. We conclude about the different criteria of the stability of $\tilde{\xi}_2$ in the following proposition.

Proposition 3. *The coexistence equilibrium point $(\tilde{\xi}_2)$ is topologically classified based on the values of $\tilde{\mathcal{D}}$, $\tilde{\mathcal{M}}$, and δ as follows:*

(1) $\tilde{\xi}_2(x^*, y^*)$ is a source:

(a) if $\tilde{\mathcal{D}}^2 - 4\tilde{\mathcal{M}} \geq 0$ and

$$\delta > \frac{-\tilde{\mathcal{D}} + \sqrt{\tilde{\mathcal{D}}^2 - 4\tilde{\mathcal{M}}}}{\tilde{\mathcal{M}}}.$$

(b) if $\tilde{\mathcal{D}}^2 - 4\tilde{\mathcal{M}} < 0$ and

$$\delta > \frac{-\tilde{\mathcal{D}}}{\tilde{\mathcal{M}}}.$$

(2) $\tilde{\xi}_2(x^*, y^*)$ is a sink:

(a) if $\tilde{\mathcal{D}}^2 - 4\tilde{\mathcal{M}} \geq 0$ and

$$\delta < \frac{-\tilde{\mathcal{D}} - \sqrt{\tilde{\mathcal{D}}^2 - 4\tilde{\mathcal{M}}}}{\tilde{\mathcal{M}}}.$$

(b) if $\tilde{\mathcal{D}}^2 - 4\tilde{\mathcal{M}} < 0$ and

$$\delta < \frac{-\tilde{\mathcal{D}}}{\tilde{\mathcal{M}}}.$$

(3) $\tilde{\xi}_2(x^*, y^*)$ is non-hyperbolic:

(a) if $\tilde{\mathcal{D}}^2 - 4\tilde{\mathcal{M}} \geq 0$ and

$$\delta = \frac{-\tilde{\mathcal{D}} \pm \sqrt{\tilde{\mathcal{D}}^2 - 4\tilde{\mathcal{M}}}}{\tilde{\mathcal{M}}}, \quad \delta \neq \frac{-2}{\tilde{\mathcal{D}}}, \frac{-4}{\tilde{\mathcal{D}}}.$$

(b) if $\tilde{\mathcal{D}}^2 - 4\tilde{\mathcal{M}} < 0$ and

$$\delta = \frac{-4}{\tilde{\mathcal{D}}}.$$

(4) $\tilde{\xi}_2(x^*, y^*)$ is a saddle in all other cases not covered above.

4. Study of bifurcations

In this section, we analyze the occurrence of NS and PD bifurcations at the fixed point $\tilde{\xi}_2(x^*, y^*)$ within the model. The parameter δ serves as a key control variable in understanding and characterizing the emergence and progression of these bifurcations.

4.1. Neimark-Sacker bifurcation

To investigate the Neimark-Sacker (NS) bifurcation, we consider δ as the bifurcation parameter. Specifically, we focus on the parameter set:

$$\widehat{\Lambda}_{\tilde{\xi}_2} = \left\{(r, m, k, \beta, p, \delta, d, \eta) \in \mathbb{R}^8_+ \mid \delta = \frac{-\tilde{\mathcal{D}}}{\tilde{\mathcal{M}}} = \delta_{NS}, \quad \frac{-\tilde{\mathcal{D}}}{\tilde{\mathcal{M}}} > 0 \quad \& \quad \tilde{\mathcal{D}}^2 - 4\tilde{\mathcal{M}} < 0\right\}.$$

This formulation describes the conditions under which the fixed point undergoes a transition to quasiperiodic behavior. Here, δ_{NS} denotes the critical bifurcation value, while the inequality ensures that the corresponding eigenvalues remain within the complex plane, maintaining stability.

By incorporating a tiny perturbation, denoted as δ^*, to the bifurcation parameter δ, we reformulate the original system (2.2) as follows:

$$\begin{aligned} x_{n+1} &= x_n + (\delta + \delta^*)\left[r x_n \left(1 - \frac{x_n}{k}\right)\frac{1}{1 + p y_n} - \frac{(1-m)x_n y_n}{\beta + (1-m)x_n}\right] \equiv f(x_n, y_n, \delta^*), \\ y_{n+1} &= y_n + (\delta + \delta^*) y_n \left[-d + \frac{\eta(1-m)x_n}{\beta + (1-m)x_n}\right] \equiv g(x_n, y_n, \delta^*). \end{aligned} \tag{4.1}$$

where (x_n, y_n) are the state variables, and δ^* serves as a perturbation to the bifurcation parameter.

To facilitate a local stability and bifurcation analysis, we introduce a coordinate transformation by defining $u_n = x_n - x^*$ and $v_n = y_n - y^*$, where (x^*, y^*) represents the equilibrium point of interest, denoted as $\tilde{\xi}_2$. This transformation effectively shifts the equilibrium to the origin, ensuring that $(u_n, v_n) = (0, 0)$ corresponds to the steady state.

To capture the local dynamics near the equilibrium, we expand $f(x_n, y_n, \delta^*)$ and $g(x_n, y_n, \delta^*)$ in a third-order Taylor series around (x^*, y^*), yielding the transformed system:

$$\begin{aligned} u_{n+1} &= \gamma_1 u_n + \gamma_2 v_n + \gamma_{11} u_n^2 + \gamma_{12} u_n v_n + \gamma_{22} v_n^2 \\ &\quad + \gamma_{111} u_n^3 + \gamma_{112} u_n^2 v_n + \gamma_{122} u_n v_n^2 + \gamma_{222} v_n^3 + O((|u_n| + |v_n|)^4), \\ v_{n+1} &= \iota_1 u_n + \iota_2 v_n + \iota_{11} u_n^2 + \iota_{12} u_n v_n + \iota_{22} v_n^2 \end{aligned} \tag{4.2}$$

$$+\iota_{111}u_n^3 + \iota_{112}u_n^2 v_n + \iota_{122}u_n v_n^2 + \iota_{222}v_n^3 + O((|u_n| + |v_n|)^4).$$

Here, the coefficients γ_i, γ_{ij}, γ_{ijk}, ι_i, ι_{ij}, and ι_{ijk} are obtained from the partial derivatives of f and g, evaluated at the equilibrium (x^*, y^*) and shown in Table 1. This expansion provides a systematic framework for studying the nonlinear behavior of the system, including bifurcations, stability transitions, and the emergence of complex dynamical phenomena.

Table 1. Coefficient values for Eq (4.2).

Term	Expression	Term	Expression
γ_1	$\frac{\delta r(k-2x^*)}{ky^*+k} + \frac{\beta\delta(m-1)y^*}{(\beta-mx^*+x^*)^2} + 1$	γ_2	$\delta\left(\frac{prx^*(x^*-k)}{k(py^*+1)^2} + \frac{(m-1)x^*}{\beta-mx^*+x^*}\right)$
γ_{11}	$\delta\left(-\frac{2r}{ky^*+k} + \frac{2(m-1)^3y^*x^*}{(\beta-mx^*+x^*)^3} + \frac{2(m-1)^2y^*}{(\beta-mx^*+x^*)^2}\right)$	γ_{12}	$\delta\left(\frac{\beta(m-1)}{(\beta-mx^*+x^*)^2} - \frac{pr(k-2x^*)}{k(py^*+1)^2}\right)$
γ_{22}	$\frac{2\delta p^2 rx^*\left(1-\frac{x^*}{k}\right)}{(py^*+1)^3}$	γ_{111}	$\frac{6\beta\delta(m-1)^3y^*}{(\beta-mx^*+x^*)^4}$
γ_{112}	$2\delta\left(\frac{pr}{k(py^*+1)^2} + \frac{(m-1)^3x^*}{(\beta-mx^*+x^*)^3} + \frac{(m-1)^2}{(\beta-mx^*+x^*)^2}\right)$	γ_{122}	$\frac{2\delta p^2 r(k-2x^*)}{k(py^*+1)^3}$
γ_{222}	$\frac{6\delta p^3 rx^*(x^*-k)}{k(py^*+1)^4}$		
ι_1	$-\frac{\beta\delta\eta(m-1)y^*}{(\beta-mx^*+x^*)^2}$	ι_2	$-d\delta - \frac{\delta\eta(m-1)x^*}{\beta-mx^*+x^*} + 1$
ι_{11}	$-\frac{2\beta\delta\eta(m-1)^2y^*}{(\beta-mx^*+x^*)^3}$	ι_{12}	$-\frac{\beta\delta\eta(m-1)}{(\beta-mx^*+x^*)^2}$
ι_{22}	0	ι_{111}	$-\frac{6\beta\delta\eta(m-1)^3y^*}{(\beta-mx^*+x^*)^4}$
ι_{112}	$-\frac{2\beta\delta\eta(m-1)^2}{(\beta-mx^*+x^*)^3}$	ι_{122}	0
ι_{222}	0		

The characteristic equation associated with system (4.2) takes the form $\nu^2 - \Lambda(\delta^*)\nu + \Upsilon(\delta^*) = 0$, where the coefficients are given by

$$\Lambda(\delta^*) = 2 + \tilde{\mathcal{D}}\delta^*, \quad \Upsilon(\delta^*) = 1 + \tilde{\mathcal{D}}\delta^* + \tilde{\mathcal{M}}(\delta^*)^2.$$

Solving for ν, the characteristic roots are expressed as:

$$\nu_{1,2}(\delta^*) = \frac{-\Lambda(\delta^*) \pm i\sqrt{4\Upsilon(\delta^*) - (\Lambda(\delta^*))^2}}{2}.$$

Imposing the condition $|\nu_{1,2}(\delta^*)| = 1$ at $\delta^* = 0$, we obtain $|\nu_{1,2}(\delta^*)| = \sqrt{\Upsilon(\delta^*)}$. Furthermore, the sensitivity of the modulus with respect to δ^* at $\delta^* = 0$ is given by

$$l = \left[\frac{d|\nu_{1,2}(\delta^*)|}{d\delta^*}\right]_{\delta^*=0} \neq 0.$$

For a bifurcation to occur, it is essential to verify that, when $\delta^* = 0$, the characteristic roots do not coincide with unity, i.e., $\nu_{1,2}^i \neq 1$ for $i = 1, 2, 3, 4$ [40]. This condition translates to the requirement

$\Lambda(0) \neq \pm 2, 0, 1$. This ensures that the system does not undergo a degenerate bifurcation scenario and maintains the integrity of its local stability analysis [41].

To derive the normal form of the system, we introduce the notations $\phi = \mathrm{Im}(\nu_{1,2})$ and $\varphi = \mathrm{Re}(\nu_{1,2})$. Utilizing the transformation matrix

$$T = \begin{bmatrix} 0 & 1 \\ \phi & \varphi \end{bmatrix},$$

we define the coordinate change

$$\begin{bmatrix} u_n \\ v_n \end{bmatrix} = T \begin{bmatrix} \overline{x}_n \\ \overline{y}_n \end{bmatrix}.$$

Substituting this transformation into system (4.2), we obtain the reformulated model:

$$\overline{x}_{n+1} = \varphi \overline{x}_n - \phi \overline{y}_n + f_{x11}(\overline{x}_n, \overline{y}_n),$$

$$\overline{y}_{n+1} = \phi \overline{x}_n + \varphi \overline{y}_n + g_{y11}(\overline{x}_n, \overline{y}_n),$$

where the nonlinear terms $f_{x11}(\overline{x}_n, \overline{y}_n)$ and $g_{y11}(\overline{x}_n, \overline{y}_n)$ represent higher-order contributions, each containing at least quadratic terms in $\overline{x}_n$ and $\overline{y}_n$.

For the system to undergo a Neimark-Sacker bifurcation, the critical parameter Ω must satisfy the non-degeneracy condition $\Omega \neq 0$. This ensures that the bifurcation is non-trivial and that the emergence of a stable or unstable invariant closed curve is governed by the system's intrinsic nonlinear dynamics.

$$\Omega = \left(\left[-Re \left[\frac{(1-2\nu_1)\nu_2^2}{1-\nu_1} \kappa_{11}\kappa_{20} \right] - \frac{1}{2}|\kappa_{11}|^2 - |\kappa_{02}|^2 + Re(\nu_2 \kappa_{21}) \right] \right)_{\delta^*=0},$$

where ν_1 and ν_2 are eigenvalues and the other coefficients are defined as follows:

$$\begin{aligned}
\kappa_{20} &= \frac{\varphi}{8}\left(2\iota_{22} - \varphi\gamma_{22} - \gamma_{12} + 4\phi\gamma_{22} + i\left(4\phi\gamma_{22} - 2\gamma_{22} - 2\varphi\gamma_{22}\right)\right) + \frac{\phi}{4}\gamma_{12} \\
&\quad + i\frac{1}{8}\left(4\phi\iota_{22} + 2\phi^2\gamma_{22} - 2\gamma_{11}\right) + \frac{\iota_{12}}{8} + \frac{\varphi\gamma_{11} - 2\iota_{11} + \varphi^3\gamma_{22} - \varphi^2\iota_{22} - \varphi^2\gamma_{12} + \varphi\iota_{12}}{4\phi}, \\
\kappa_{11} &= \frac{\phi}{2}(\iota_{22} - \varphi\gamma_{22}) + i\frac{1}{2}(\phi^2\gamma_{22} + \gamma_{11} + \varphi\gamma_{12} + \varphi^2\gamma_{22}) \\
&\quad + \frac{\iota_{11} - \varphi\gamma_{11} + \varphi\iota_{12} - \varphi^2\gamma_{12} - 2\varphi^2\iota_{22} + 2\varphi^3\gamma_{22}}{2\phi}, \\
\kappa_{02} &= \frac{1}{4}\phi(2\varphi\gamma_{22} + \gamma_{12} + \iota_{22}) + i\frac{1}{4}(\iota_{12} + 2\varphi\iota_{22} - 2\varphi\gamma_{12} - \gamma_{11}) \\
&\quad - \frac{\iota_{11} - \varphi\gamma_{11} + \varphi\iota_{12} - \varphi^2\gamma_{12} + \varphi^2\iota_{22} - \varphi^3\gamma_{22}}{4\phi} + \frac{1}{4}\gamma_{22}i(\phi^2 - 3\varphi^2), \\
\kappa_{21} &= \frac{3}{8}\iota_{222}(\phi^2 + \varphi^2) + \frac{\iota_{112}}{8} + \frac{\varphi}{4}\gamma_{112} + \frac{\varphi}{4}\iota_{122} + \gamma_{122}\left(\frac{\phi^2}{8} + \frac{3\varphi^2}{8} - \frac{\varphi}{4}\right)
\end{aligned}$$

$$+\frac{3}{8}\gamma_{111}+i\frac{3}{8}\gamma_{222}(\phi^2+2\varphi^2)+i\frac{3\phi\varphi}{8}\gamma_{122}-\frac{1}{8}\iota_{122}\phi i-i\frac{3\phi\varphi}{8}\iota_{222}-i\frac{3\iota_{111}-3\varphi\gamma_{111}}{8\phi}$$
$$-i\frac{3\varphi\iota_{112}-3\varphi^2\gamma_{112}}{8\phi}-i\frac{3\varphi^2\iota_{122}-3\varphi^3\gamma_{122}}{8\phi}-i\frac{3\varphi^3\iota_{222}-3\varphi^4\gamma_{222}}{8\phi}.$$

Theorem 1. *An NS bifurcation occurs at the equilibrium $\tilde{\xi}_2(x^*,y^*)$ when the parameter δ reaches the critical threshold $\widehat{\Lambda}_{\tilde{\xi}_2}$, provided $\Omega\neq 0$.*

(i) If $\Omega<0$, the bifurcation is subcritical, producing a closed invariant curve around $\tilde{\xi}_2$.

(ii) If $\Omega>0$, the bifurcation is supercritical, also leading to an invariant curve.

4.2. Period-doubling bifurcation

Here, we delve into the period-doubling (PD) bifurcation by employing δ as the bifurcation parameter. In particular, we define the critical parameter set as:

$$\widehat{\Theta}_{\tilde{\xi}_2}=\left\{(r,m,k,\beta,p,\delta,d,\eta)\in\mathbb{R}^8_+\mid \delta=\frac{-\tilde{\mathcal{D}}\pm\sqrt{\tilde{\mathcal{D}}^2-4\tilde{\mathcal{M}}}}{\tilde{\mathcal{M}}}=\delta_{\pm},\quad \tilde{\mathcal{D}}^2-4\tilde{\mathcal{M}}\geq 0,\quad \delta\neq\frac{-2}{\tilde{\mathcal{D}}},\frac{-4}{\tilde{\mathcal{D}}}\right\}.$$

This condition delineates the onset of period-doubling bifurcation, where the fixed point destabilizes, giving rise to a sequence of period-doubled orbits. To rigorously track this bifurcation, we introduce a small perturbation δ^* to the bifurcation parameter δ. The introduction of the perturbed parameter modifies the original system given in model (2.2), which now takes the form

$$\begin{aligned}x_{n+1}&=x_n+(\delta+\delta^*)\left[rx_n\left(1-\frac{x_n}{k}\right)\frac{1}{1+py_n}-\frac{(1-m)x_ny_n}{\beta+(1-m)x_n}\right]\equiv f(x_n,y_n,\delta^*),\\ y_{n+1}&=y_n+(\delta+\delta^*)y_n\left[-d+\frac{\eta(1-m)x_n}{\beta+(1-m)x_n}\right]\equiv g(x_n,y_n,\delta^*),\end{aligned}\tag{4.3}$$

To facilitate a local stability and bifurcation analysis, we introduce the transformations $u_n=x_n-x^*$ and $v_n=y_n-y^*$, where (x^*,y^*) denotes the equilibrium point $\tilde{\xi}_2(x^*,y^*)$. Shifting the coordinate system so that the equilibrium coincides with the origin, we expand the nonlinear terms in f and g as a third-order Taylor series about $(0,0,0)$. This yields the following transformed system:

$$\begin{aligned}u_{n+1}&=\gamma_1u_n+\gamma_2v_n+\gamma_{11}u_n^2+\gamma_{12}u_nv_n+\gamma_{13}u_n\delta^*+\gamma_{23}v_n\delta^*+\gamma_{111}u_n^3+\\&\quad\gamma_{112}u_n^2v_n+\gamma_{113}u_n^2\delta^*+\gamma_{123}u_nv_n\delta^*+O((|u_n|+|v_n|+|\delta^*|)^4),\\ v_{n+1}&=\iota_1u_n+\iota_2v_n+\iota_{11}u_n^2+\iota_{12}u_nv_n+\iota_{22}v_n^2+\iota_{13}u_n\delta^*+\iota_{23}v_n\delta^*+\iota_{111}u_n^3+\\&\quad\iota_{112}u_n^2v_n+\iota_{113}u_n^2\delta^*+\iota_{123}u_nv_n\delta^*+\iota_{223}v_n^2\delta^*+O((|u_n|+|v_n|+|\delta^*|)^4),\end{aligned}\tag{4.4}$$

where all the coefficients of system (104) are displayed in Table 2.

Table 2. Coefficient values for Eq (4.4).

Term	Expression	Term	Expression
γ_{13}	$\frac{r(k-2x^*)}{kpy^*+k}+\frac{\beta(m-1)y^*}{(\beta-mx^*+x^*)^2}$	γ_{23}	$\frac{prx^*(x^*-k)}{k(py^*+1)^2}+\frac{(m-1)x^*}{\beta-mx^*+x^*}$
γ_{113}	$-\frac{2r}{kpy^*+k}+\frac{2(m-1)^3y^*x^*}{(\beta-mx^*+x^*)^3}+\frac{2(m-1)^2y^*}{(\beta-mx^*+x^*)^2}$	γ_{123}	$\frac{\beta(m-1)}{(\beta-mx^*+x^*)^2}-\frac{pr(k-2x^*)}{k(py^*+1)^2}$
ι_{13}	$-\frac{\beta\eta(m-1)y^*}{(\beta-mx^*+x^*)^2}$	ι_{23}	$-d-\frac{\eta(m-1)x^*}{\beta-mx^*+x^*}$
ι_{113}	$-\frac{2\beta\eta(m-1)^2y^*}{(\beta-mx^*+x^*)^3}$	ι_{123}	$-\frac{\beta\eta(m-1)}{(\beta-mx^*+x^*)^2}$
ι_{223}	0		

Let $T = \begin{bmatrix} \gamma_2 & \gamma_2 \\ -1-\gamma_1 & \nu_2-\gamma_1 \end{bmatrix}$ be an invertible transformation matrix. By applying the change of variables $\begin{bmatrix} u_n \\ v_n \end{bmatrix} = T \begin{bmatrix} \overline{x}_n \\ \overline{y}_n \end{bmatrix}$, the original system in model (4.4) is reformulated into the following canonical form:

$$\begin{aligned} \overline{x}_{n+1} &= -\overline{x}_n + f_{x11}(u_n, v_n, \delta^*), \\ \overline{y}_{n+1} &= \nu_2 \overline{y}_n + g_{y11}(u_n, v_n, \delta^*). \end{aligned} \tag{4.5}$$

Here, the transformed state variables $(\overline{x}_n, \overline{y}_n)$ encapsulate the essential dynamics of the original system, with f_{x11} and g_{y11} incorporating nonlinear perturbations. The transformation preserves the rank of the system at a minimum of two, ensuring that its fundamental structural properties remain intact.

A critical consequence of this formulation is the existence of a center manifold $W^c(0,0,0)$ near the equilibrium $(0,0)$, under the assumption that the bifurcation parameter δ^* is sufficiently small. This result follows directly from the center manifold theorem, which facilitates the reduction of the system to its most relevant dynamical components. Consequently, the long-term behavior of the system can be effectively described by the reduced manifold approximation [10]:

$$W^c(0,0,0) = \left\{ (\overline{x}_n, \overline{y}_n, \delta^*) \in \mathbb{R}^3 : \overline{y}_{n+1} = \overline{\gamma}_1 \overline{x}_n^2 + \overline{\gamma}_2 \overline{x}_n \delta^* + O((|\overline{x}_n| + |\delta^*|)^3) \right\}.$$

This reduced representation captures the dominant nonlinear interactions governing the system's dynamics, providing a rigorous foundation for bifurcation analysis and stability investigations.

The coefficients governing the reduced dynamics, $\overline{\gamma}_1$ and $\overline{\gamma}_2$, are explicitly given by

$$\begin{aligned} \overline{\gamma}_1 &= \frac{\gamma_2[(1+\gamma_1)\gamma_{11} + \gamma_2\gamma_{11}]}{1-\nu_2^2} + \frac{\iota_{22}(1+\gamma_1)^2}{1-\nu_2^2} - \frac{(1+\gamma_1)[\gamma_{12}(1+\gamma_1) + \gamma_2\iota_{12}]}{1-\nu_2^2}, \\ \overline{\gamma}_2 &= \frac{(1+\gamma_1)[\gamma_{23}(1+\gamma_1) + \gamma_2\iota_{23}]}{\gamma_2(1+\nu_2)^2} - \frac{(1+\gamma_1)[\gamma_{13} + \gamma_2\iota_{13}]}{(1+\nu_2)^2}. \end{aligned}$$

These coefficients encapsulate the nonlinear interactions governing the system's behavior near the center manifold, incorporating contributions from both direct and indirect variable dependencies. The inclusion of higher-order terms refines the approximation, allowing for a more precise characterization of the local dynamics.

The evolution of $\overline{x}_n$ follows the recurrence relation

$$\overline{x}_{n+1} = -\overline{x}_n + \sigma_1 \overline{x}_n^2 + \sigma_2 \overline{x}_n \delta^* + \sigma_3 \overline{x}_n^2 \delta^* + \sigma_4 \overline{x}_n \delta^{*2} + \sigma_5 \overline{x}_n^3 + O((|\overline{x}_n| + |\delta^*|)^4) \equiv F(\overline{x}_n, \delta^*).$$

Here, the coefficients $\sigma_1, \sigma_2, \sigma_3, \sigma_4,$ and σ_5 capture the essential nonlinear effects shaping the system's dynamics near equilibrium. These terms not only determine the nature of local bifurcations, but also influence the stability and persistence of equilibrium states. Higher-order corrections further refine the analysis, ensuring a comprehensive representation of the system's response to perturbations

in both $\overline{x}_n$ and δ^*. Consider

$$\begin{aligned}
\sigma_1 &= \frac{\overline{\gamma}_2[(\nu_2-\overline{\gamma}_1)\gamma_{11}-\overline{\gamma}_2\iota_{11}]}{1+\nu_2}-\frac{\iota_{22}(1+\overline{\gamma}_1)^2}{1+\nu_2}-\frac{(1+\overline{\gamma}_1)[(\nu_2-\overline{\gamma}_1)\gamma_{12}-\overline{\gamma}_2\iota_{12}]}{1+\nu_2},\\
\sigma_2 &= \frac{(\nu_2-\overline{\gamma}_1)\gamma_{13}-\overline{\gamma}_2\iota_{13}}{1+\nu_2}-\frac{(1+\overline{\gamma}_1)[(\nu_2-\overline{\gamma}_1)\gamma_{23}-\overline{\gamma}_2\iota_{23}]}{\overline{\gamma}_2(1+\nu_2)},\\
\sigma_3 &= \frac{(\nu_2-\gamma_1)\overline{\gamma}_1\gamma_{13}-\gamma_2\iota_{13}}{1+\nu_2}+\frac{[(\nu_2-\gamma_1)\gamma_{23}-\gamma_2\iota_{23}](\nu_2-\gamma_1)\overline{\gamma}_1}{\gamma_2(1+\nu_2)}\\
&\quad-\frac{(1+\gamma_1)[(\nu_2-\gamma_1)\gamma_{123}-\gamma_2\iota_{123}]}{1+\nu_2}+\frac{\gamma_2[(\nu_2-\gamma_1)\gamma_{113}-\gamma_2\iota_{113}]}{1+\nu_2}\\
&\quad-\frac{\iota_{223}(1+\gamma_1)^2}{1+\nu_2}+\frac{2\gamma_2\overline{\gamma}_2[(\nu_2-\gamma_1)\gamma_{11}-\gamma_2\iota_{11}]}{1+\nu_2}\\
&\quad-\frac{2\iota_{22}\overline{\gamma}_2(1+\gamma_1)(\nu_2-\gamma_1)}{1+\nu_2}+\frac{\overline{\gamma}_2[(\nu_2-\gamma_1)\gamma_{12}-\gamma_2\iota_{12}](\nu_2-1-2\gamma_1)}{1+\nu_2},\\
\sigma_4 &= \frac{\overline{\gamma}_2[(\nu_2-\gamma_1)\gamma_{13}-\gamma_2\iota_{13}]}{1+\nu_2}+\frac{[(\nu_2-\gamma_1)\gamma_{23}-\gamma_2\iota_{23}](\nu_2-\gamma_1)\overline{\gamma}_2}{\gamma_2(1+\nu_2)}\\
&\quad+\frac{2\gamma_2\overline{\gamma}_2[(\nu_2-\gamma_1)\gamma_{11}-\gamma_2\iota_{11}]}{1+\nu_2}\\
&\quad+\frac{2\iota_{22}\overline{\gamma}_2(1+\gamma_1)(\nu_2-\gamma_1)}{1+\nu_2}+\frac{\overline{\gamma}_2[(\nu_2-\gamma_1)\gamma_{12}-\gamma_2\iota_{12}](\nu_2-1-2\gamma_1)}{1+\nu_2},\\
\sigma_5 &= \frac{2\gamma_2\overline{\gamma}_1[(\nu_2-\gamma_1)\gamma_{11}-\gamma_2\iota_{11}]}{1+\nu_2}+\frac{[(\nu_2-\gamma_1)\gamma_{11}-\gamma_2\iota_{11}](\nu_2-1-2\gamma_1)\overline{\gamma}_1}{1+\nu_2}\\
&\quad+\frac{2\iota_{22}\overline{\gamma}_1(\nu_2-\gamma_1)(1+\gamma_1)}{1+\nu_2}+\frac{\overline{\gamma}_2^2[(\nu_2-\gamma_1)\gamma_{111}-\gamma_2\iota_{111}]}{1+\nu_2}\\
&\quad-\frac{\overline{\gamma}_2(1+\gamma_1)[(\nu_2-\gamma_1)\gamma_{112}-\gamma_2\iota_{112}]}{1+\nu_2}.
\end{aligned}$$

A period-doubling (PD) bifurcation occurs when the critical quantities ϖ_1 and ϖ_2 are both nonzero [10]. These key parameters are defined as follows:

$$\varpi_1 = \left(\frac{\partial^2 F}{\partial\overline{x}\partial\delta^*}+\frac{1}{2}\frac{\partial F}{\partial\delta^*}\frac{\partial^2 F}{\partial\overline{x}^2}\right)\Big|_{(0,0)},$$

which measures the sensitivity of the system's response to variations in the bifurcation parameter δ^*, and

$$\varpi_2 = \left(\frac{1}{6}\frac{\partial^3 F}{\partial\overline{x}^3}+\left(\frac{1}{2}\frac{\partial^2 F}{\partial\overline{x}^2}\right)^2\right)\Big|_{(0,0)},$$

which quantifies the influence of cubic nonlinearities on the bifurcation structure. The nonzero values of ϖ_1 and ϖ_2 ensure that the system undergoes a period-doubling transition, leading to qualitative changes in its dynamical behavior [10].

The following theorem formalizes the criteria and implications of the period-doubling (PD) bifurcation.

Theorem 2. *A period-doubling bifurcation emerges at the equilibrium $\tilde{\xi}_2(x^*, y^*)$ when the bifurcation parameter μ is within a defined neighborhood of $\widehat{\Theta}_{\tilde{\xi}_2}$. This bifurcation is assured provided that both critical conditions $\varpi_1 \neq 0$ and $\varpi_2 \neq 0$ hold. The stability characteristics of the newly formed period-two orbits hinge on the sign of ϖ_2: If $\varpi_2 > 0$, the resulting periodic orbits are stable; conversely, if $\varpi_2 < 0$, they exhibit instability.*

5. Numerical results and discussion

In this section, we choose parameter values based on hypothetical but biologically plausible assumptions to carry out numerical simulations. These parameters are grounded in ecologically or physiologically realistic conditions, ensuring the outcomes remain applicable to actual biological systems.

5.1. NS bifurcation simulation

Building on our previous analysis of the critical role played by the parameter δ in inducing a Neimark–Sacker (NS) bifurcation, we now shift our attention to the intricate evolution of the system's dynamics beyond this bifurcation point. By systematically varying key parameters, such as p or δ, while holding others fixed, we seek to elucidate the emergent dynamical regimes and their ecological implications.

For the discrete prey-predator model (2.2), we consider the parameter set

$$(r, m, k, \beta, p, d, \eta) = (2.2, 0.45, 1.65, 1.1, 1.1, 0.21, 0.85)$$

with initial conditions $(x_0, y_0) = (0.65, 1.39)$. The bifurcation parameter δ is varied over the interval $[1.4, 2.8]$, and at the critical threshold $\delta = 1.62899$, the system undergoes a Neimark–Sacker bifurcation. The positive equilibrium of the system is given by $\tilde{\xi}_2 = (0.65625, 1.39104)$, and the Jacobian matrix evaluated at this point yields the characteristic polynomial

$$J(\nu) = \nu^2 - 1.64743\nu + 0.999999.$$

The corresponding eigenvalues, $\nu_{1,2} = 0.823714 \pm 0.567004i$, have a modulus of $|\nu_{1,2}| = 1$ precisely at $\delta = 1.62899$, thereby confirming the onset of the NS bifurcation. This transition marks the emergence of quasiperiodic oscillations, paving the way for increasingly complex dynamical behaviors as δ is further varied.

Figures 1(a) and (b) illustrate the bifurcation structure of the system over the range $\delta \in [1.4, 2.8]$, while Figure 1(c) provides a local amplification within $[2.3, 2.65]$. Additionally, Figure 1(d) depicts the maximum Lyapunov exponents, pinpointing the NS bifurcation precisely at $\delta = 1.62899$.

The bifurcation diagrams for prey (x) and predator (y) populations reveal a transition from a stable equilibrium at lower δ values to quasi-periodic oscillations as δ surpasses the critical threshold. The emergence of a toroidal structure in phase space confirms the onset of a Neimark–Sacker bifurcation (see Figure 2(a) for the case $\delta = 1.635$). With increasing δ, the system undergoes secondary bifurcations, eventually exhibiting periodic and chaotic attractors. At sufficiently high δ, the bifurcation diagram displays a dense scattering of points, characteristic of chaotic dynamics with extreme sensitivity to initial conditions.

Phase portraits in Figure 2(a) for selected δ values further illustrate this dynamical evolution, highlighting transitions from fixed points to quasi-periodic and periodic attractors. Distinct periodic structures are observed at $\delta = 1.789$, 1.956, and 2.23. Meanwhile, Figure 2(b) integrates these phase portraits into a 3D representation of the x-y-δ parameter space, offering a comprehensive visualization of system transitions.

These findings underscore the system's rich dynamical behavior, tracing its progression from equilibrium to complex oscillatory states and chaos. The analysis provides critical insights into the interplay between stability and complexity in discrete ecological models, with broader implications for understanding non-linear phenomena in predator-prey interactions and other applied contexts.

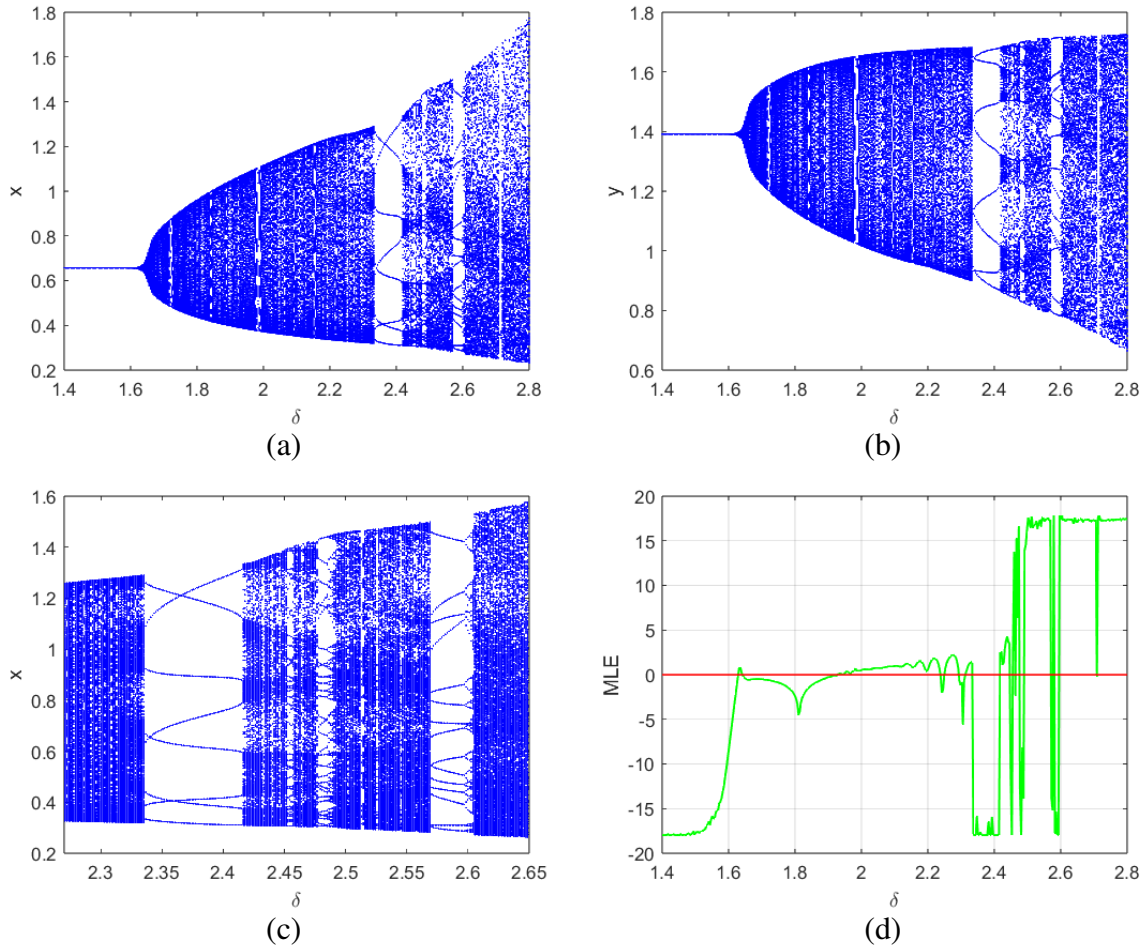

Figure 1. Visualization of bifurcation (NS) diagram of system (2.2) with local amplification and maximum lyapunov exponents for $r = 2.2$, $k = 1.65$, $p = 1.1$, $\beta = 1.1$, $m = 0.45$, $\eta = 0.85$, $d = 0.21$, initial conditions $(x_0, y_0) = (0.65, 1.39)$, and δ varies in $[1.4, 2.8]$, (a) prey population, (b) predator population, (c) local amplification, (d) MLEs.

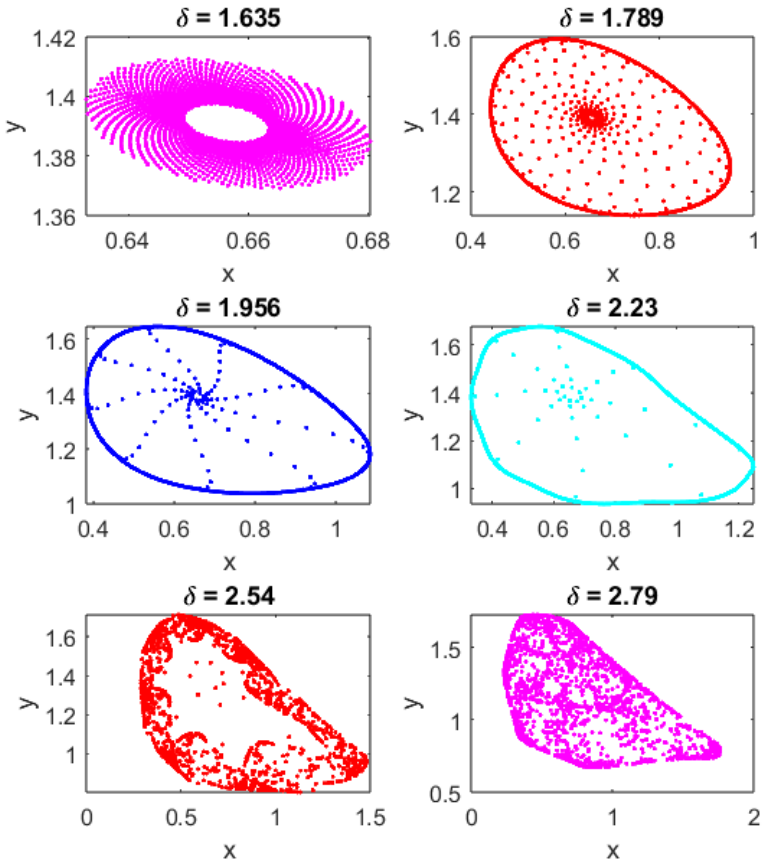

(a)

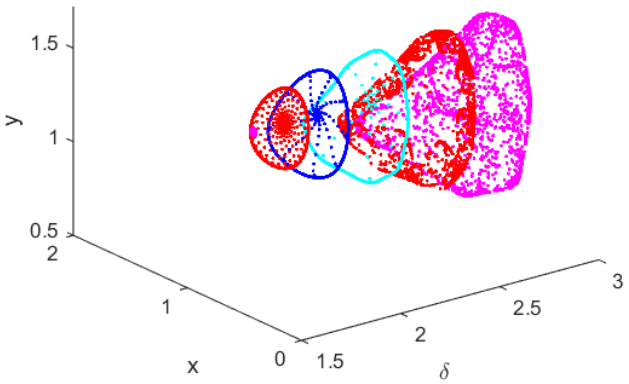

(b)

Figure 2. (a) Phase portrait for NS bifurcation for different values of δ. (b) 3D representation of phase portraits corresponding to Figure 2 (a).

Figures 3(a) and (b) present the bifurcation diagram for $p \in [0.8, 2.4]$, while Figure 3(c) depicts

the corresponding maximum Lyapunov exponents, precisely identifying the NS bifurcation at $p = 1.1052$. Phase portraits in Figure 4(a) illustrate the repelling nature of the fixed point and periodic structures at $p = 1.035$, 1.45, and 1.72, while Figure 4(b) integrates these into a three-dimensional x-y-p representation, capturing the system's transition from stability to chaotic dynamics.

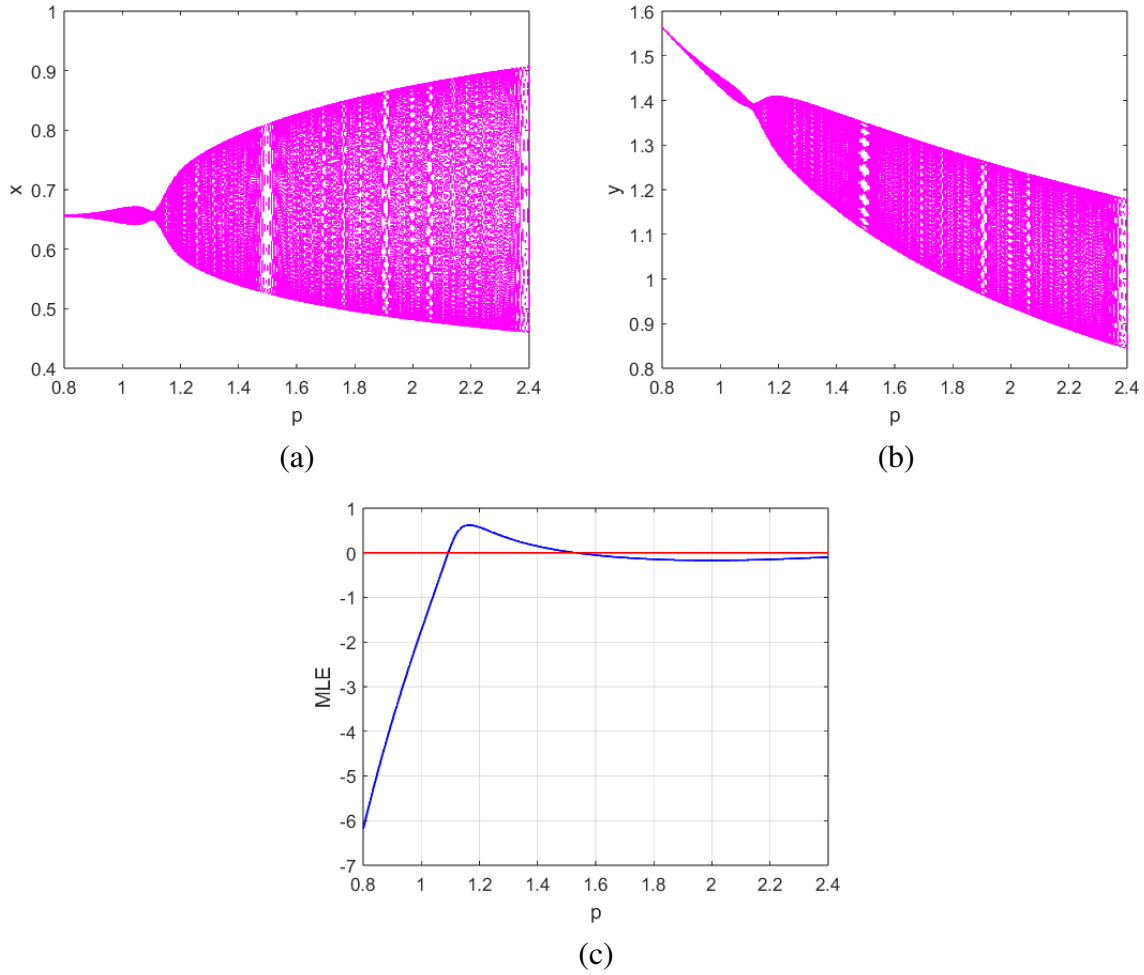

Figure 3. Visualisation of bifurcation (NS) diagram of system (2.2) and maximum lyapunov exponent for $r = 2.2$, $k = 1.65$, $\delta = 1.62889$, $\beta = 1.1$, $m = 0.45$, $\eta = 0.85$, $d = 0.21$, initial conditions $(x_0, y_0) = (0.65, 1.39)$, and p varies in $[0.8, 2.4]$, (a) prey population, (b) predator population, (c) MLEs.

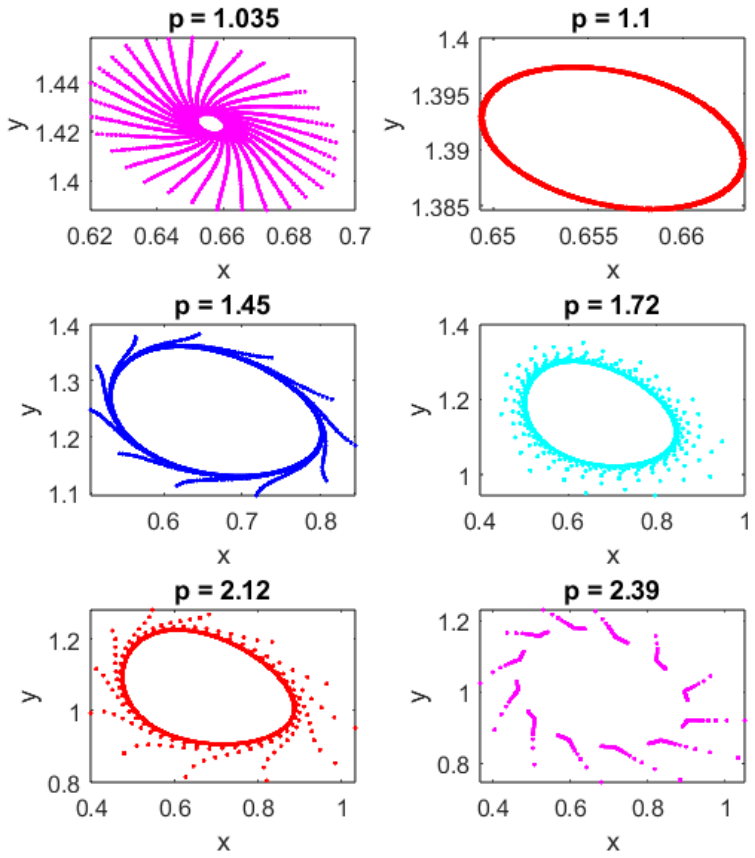

(a)

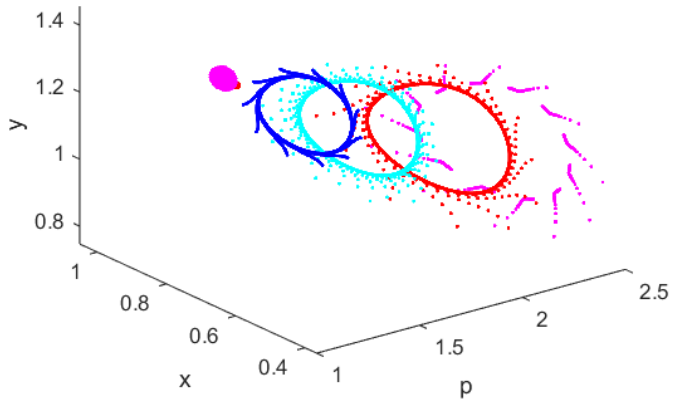

(b)

Figure 4. (a) Phase portrait for NS bifurcation for different values of p. (b) 3D representation of phase portraits corresponding to Figure 4 (a).

Further insights are provided by 3D bifurcation diagrams in Figures 5(a) and (b), alongside two- and

three-dimensional visualizations of the maximum Lyapunov exponent (Figures 5(c) and (d)), detailing dynamical transitions over $p \in [0.8, 2.4]$ and $\delta \in [1.4, 2.8]$.

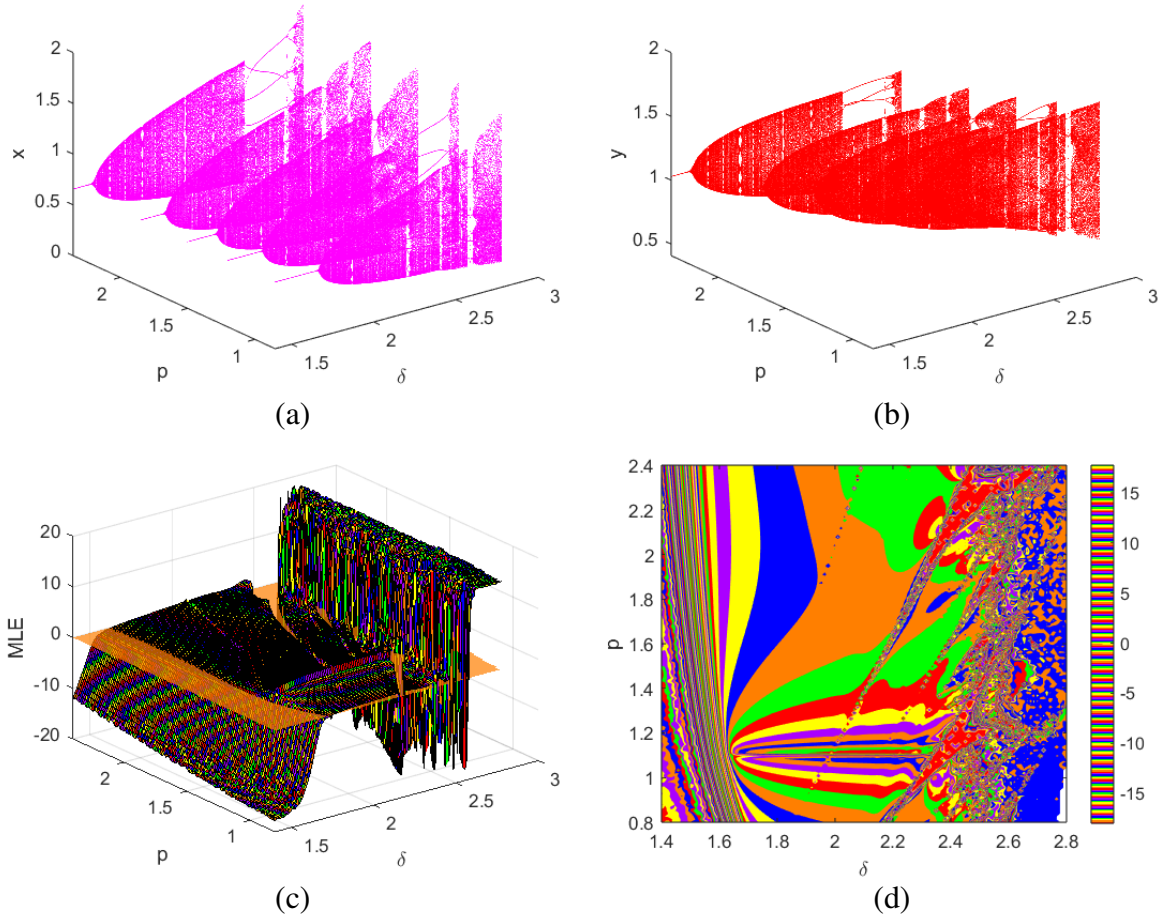

Figure 5. (a) and (b): 3D representation of Neimark-Sacker (NS) bifurcation diagrams for prey and predator populations by varying the two bifurcation parameters δ and p; (c) and (d): 3D & 2D maximal Lyapunov exponents.

The three-dimensional bifurcation diagrams provide an in-depth illustration of how the system responds to varying parameters, offering critical insights into the dynamics of predator-prey interactions. These visualizations help pinpoint specific parameter intervals that result in a range of behaviors, including equilibrium states, periodic oscillations, and chaotic dynamics, thereby deepening our comprehension of the system's complexity. The intricate patterns of folding and stretching seen on the maximum lyapunov exponent (MLE) surface emphasize the system's pronounced sensitivity to parameter alterations. To facilitate clearer interpretation, a two-dimensional projection of the MLE surface is also included. This simplified representation effectively highlights key parameter zones associated with distinct dynamic regimes, such as stability, periodicity, and chaos. Despite the reduction in dimensionality, the 2D plot preserves vital structural features, capturing the essential transitions in behavior. The integration of both 3D and 2D visual tools provides a comprehensive

understanding of the model, illustrating how parameter variations in δ and p drive the onset of complex, chaotic patterns in predator-prey population dynamics. These representations offer a refined perspective on orbital structures and local MLE variations. Consistent with the analysis in Section 4, these findings reinforce a comprehensive understanding of NS bifurcations, illustrating the system's sensitivity to parameter perturbations and its ecological implications. The results indicate that the fear effect can influence the system in both stabilizing and destabilizing ways. Specifically, when fear intensity remains at a moderate level, it tends to promote the coexistence of predator and prey populations, as reflected by the emergence of bifurcation phenomena.

6. Chaos control

In discrete-time dynamical systems, chaos control is typically implemented through four principal methodologies: state feedback control, the Ott-Grebogi-Yorke (OGY) method, pole-placement control, and hybrid strategies. Among these, state feedback control and the OGY method are the most widely utilized approaches [41–44].

6.1. OGY method of controling chaos

This subsection focuses on the OGY method, which eliminates chaotic behavior by making small, strategic perturbations to system parameters, thereby steering the system toward a desired stable orbit.

The discrete prey-predator system in Eq (2.2) can be expressed in the following form:

$$\begin{aligned} x_{n+1} &= x_n + \delta\left[rx_n\left(1-\frac{x_n}{k}\right)\frac{1}{1+py_n} - \frac{(1-m)x_ny_n}{\beta+(1-m)x_n}\right] \equiv f(x_n, y_n, p), \\ y_{n+1} &= y_n + \delta y_n\left[-d + \frac{\eta(1-m)x_n}{\beta+(1-m)x_n}\right] \equiv g(x_n, y_n, p). \end{aligned} \tag{6.1}$$

To impose chaotic behaviors, we introduce p as a control parameter, enforcing the constraint $|p - p_0| < \tilde{\delta}$, where $\tilde{\delta} > 0$ and p_0 denotes a small value within the chaotic regime. A feedback control mechanism is implemented to move the system toward the targeted stable orbit. When the system initially resides in an unstable state, its approximate behavior, as characterized by Eq (2.1), can be effectively described by the following linear mapping:

$$\begin{bmatrix} x_{n+1}-x^* \\ y_{n+1}-y^* \end{bmatrix} \approx A \begin{bmatrix} x_n-x^* \\ y_n-y^* \end{bmatrix} + B\left[p-p_0\right], \tag{6.2}$$

where

$$\begin{aligned} A_{(x^*,y^*,p)} &= \begin{bmatrix} \frac{\partial f(x^*,y^*,p)}{\partial x} & \frac{\partial f(x^*,y^*,p)}{\partial y} \\ \frac{\partial g(x^*,y^*,p)}{\partial x} & \frac{\partial g(x^*,y^*,p)}{\partial y} \end{bmatrix} \\ &= \begin{bmatrix} \frac{\delta r(k-2x^*)}{kpy^*+k} + \frac{\beta\delta(m-1)y^*}{(\beta-mx^*+x^*)^2} + 1 & \delta\left(\frac{prx^*(x^*-k)}{k(py^*+1)^2} + \frac{(m-1)x^*}{\beta-mx^*+x^*}\right) \\ -\frac{\beta\delta\eta(m-1)y^*}{(\beta-mx^*+x^*)^2} & -d\delta - \frac{\delta\eta(m-1)x^*}{\beta-mx^*+x^*} + 1 \end{bmatrix}, \end{aligned}$$

and

$$B_{(x^*,y^*,p)} = \begin{bmatrix} \frac{\partial f(x^*,y^*,p)}{\partial p} \\ \frac{\partial g(x^*,y^*,p)}{\partial p} \end{bmatrix} = \begin{bmatrix} \frac{\delta rx^*y^*(x^*-k)}{k(py^*+1)^2} \\ 0 \end{bmatrix}.$$

The controllability of system (6.1) is examined concerning the matrix C provided below:

$$C = \left[B_{(x^*,y^*,p)} : A_{(x^*,y^*,p)}B_{(x^*,y^*,p)}\right]$$

$$= \begin{bmatrix} \frac{\delta r x^* y^*(x^*-k)}{k(py^*+1)^2} & -\frac{\delta r x^* y^*\left(1-\frac{x^*}{k}\right)\left(\delta\left(\frac{r\left(1-\frac{x^*}{k}\right)}{py^*+1}-\frac{rx^*}{k(py^*+1)}+\frac{(1-m)^2x^*y^*}{(\beta+(1-m)x^*)^2}-\frac{(1-m)y^*}{\beta+(1-m)x^*}\right)+1\right)}{(py^*+1)^2} \\ 0 & -\frac{\delta^2 r x^* y^{*2}\left(1-\frac{x^*}{k}\right)\left(\frac{\eta(1-m)}{\beta+(1-m)x^*}-\frac{\eta(1-m)^2x^*}{(\beta+(1-m)x^*)^2}\right)}{(py^*+1)^2} \end{bmatrix},$$

The controllability matrix C has a rank of 2, ensuring that the system is fully controllable. To ensure that the equilibrium solution of the Eq (6.2) remains locally asymptotically stable, all eigenvalues of the matrix $A - BK$ must reside strictly within the open unit disk in the complex plane. If this requirement is not met, the solution becomes unstable, making it unsuitable for further analysis. By implementing the feedback control law

$$[p - p_0] = -K\begin{bmatrix} x_n - x^* \\ y_n - y^* \end{bmatrix},$$

where $K = \begin{bmatrix} d_1 & d_2 \end{bmatrix}$, the system dynamics governed by Eq (6.2) can be reformulated to express the closed-loop behavior as follows:

$$\begin{bmatrix} x_{n+1} - x^* \\ y_{n+1} - y^* \end{bmatrix} \approx [A - BK]\begin{bmatrix} x_n - x^* \\ y_n - y^* \end{bmatrix}. \tag{6.3}$$

Here,

$$A - BK = \begin{bmatrix} F_{11} & F_{12} \\ F_{21} & F_{22} \end{bmatrix}. \tag{6.4}$$

Consider,

$$F_{11} = \frac{\delta d_1 r x^* y^*\left(1-\frac{x^*}{k}\right)}{(py^*+1)^2} + \delta\left(\frac{r\left(1-\frac{x^*}{k}\right)}{py^*+1} - \frac{rx^*}{k(py^*+1)} + \frac{(1-m)^2x^*y^*}{(\beta+(1-m)x^*)^2} - \frac{(1-m)y^*}{\beta+(1-m)x^*}\right) + 1,$$

$$F_{12} = \frac{\delta d_2 r x^* y^*\left(1-\frac{x^*}{k}\right)}{(py^*+1)^2} + \delta\left(-\frac{prx^*\left(1-\frac{x^*}{k}\right)}{(py^*+1)^2} - \frac{(1-m)x^*}{\beta+(1-m)x^*}\right),$$

$$F_{21} = \delta y^*\left(\frac{\eta(1-m)}{\beta+(1-m)x^*} - \frac{\eta(1-m)^2x^*}{(\beta+(1-m)x^*)^2}\right),$$

$$F_{22} = \delta\left(\frac{\eta(1-m)x^*}{\beta+(1-m)x^*} - d\right) + 1.$$

The characteristic equation is written as:

$$A(\nu) = \nu^2 - \Lambda\nu + \Upsilon = 0, \tag{6.5}$$

where ν_1 and ν_2 denote the roots of Eq (6.5). The parameters Λ and Υ, corresponding to the trace and determinant of the matrix $A - BK$, are defined as:

$$\Lambda = F_{11} + F_{22}, \quad \Upsilon = F_{11}F_{22} - F_{12}F_{21}.$$

To delineate the boundaries of marginal stability, the conditions $\nu_1 = \pm 1$ and $\nu_1\nu_2 = 1$ must hold. These constraints ensure that both eigenvalues, ν_1 and ν_2, remain strictly within the open unit disk in the complex plane, thereby preserving system stability. In particular, the condition $\nu_1\nu_2 = 1$ provides critical insights into the system's stability characteristics and dynamic transitions. This analytical formulation serves as the foundation for examining stability margins and the onset of instability.

The conditions $\nu_1 = \pm 1$ and $\nu_1\nu_2 = 1$ serve as the basis for deriving equations that define the boundaries of marginal stability, ensuring that both eigenvalues remain strictly within the open unit disk [44]. By systematically evaluating the cases $\nu_1\nu_2 = 1$, $\nu_1 = -1$, and $\nu_1 = 1$, the characteristic Eq (6.5) yields the following stability boundary equations:

$$\begin{aligned} L_1 &= \Upsilon - 1, \\ L_2 &= \Lambda - \Upsilon - 1, \\ L_3 &= 1 + \Lambda + \Upsilon. \end{aligned} \tag{6.6}$$

Under specific parameter constraints, the stable eigenvalues are confined within a triangular region in the d_1d_2 plane, delineated by the lines L_1, L_2, and L_3. This triangular domain represents the region of stability, determined by the intersection of these boundary conditions.

Illustration: Consider the parameter set

$$(\delta, r, m, k, \beta, p_0, d, \eta) = (1.62889, 2.2, 0.45, 1.65, 1.1, 1.09, 0.21, 0.85)\,.$$

For the system (2.2), a coexistence equilibrium is identified at $\{x \to 0.65625, y \to 1.39056\}$. The modified system dynamics are governed by the recurrence relations:

$$\begin{aligned} x_{n+1} &= 1.62889\left(\frac{2.2(1 - 0.606061x_n)x_n}{1.101y_n + 1} - \frac{0.55x_ny_n}{0.55x_n + 1.1}\right) + x_n, \\ y_{n+1} &= 1.62889\left(\frac{0.4675x_n}{0.55x_n + 1.1} - 0.21\right)y_n + y_n. \end{aligned} \tag{6.7}$$

The system's stability boundaries, delineated by the lines L_1, L_2, and L_3, are defined as follows:

$$L_1 = 0.307454d_1 - 0.167793d_2 + 0.0000287615 = 0,$$

$$L_2 = -0.167793d_2 + 0.35248 = 0,$$

$$L_3 = 0.614908d_1 - 0.167793d_2 + 3.64758 = 0.$$

These boundaries enclose a triangular stability region, depicted in Figure 6, which characterizes the domain where the eigenvalues remain within the stability criterion. This figure provides a graphical representation of the stable eigenvalue region for the controlled system described by Eq (6.7), obtained using the Ott-Grebogi-Yorke (OGY) control method.

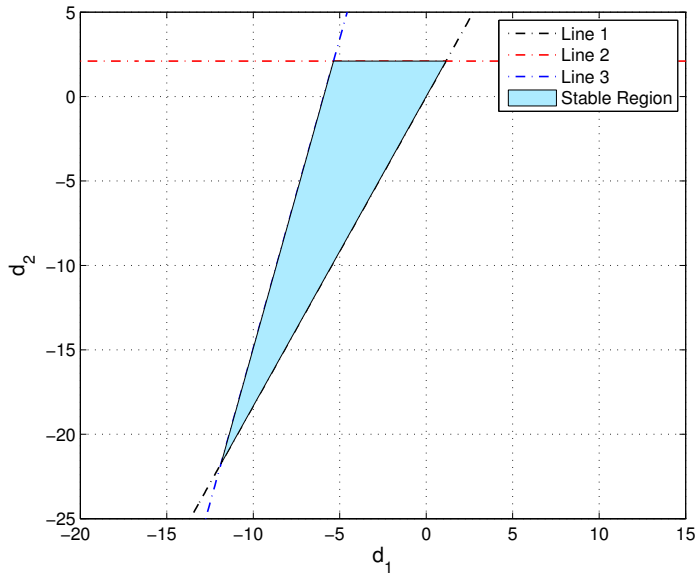

Figure 6. Stable eigenvalue region determined via the OGY control method.

6.2. State feedback control method

State feedback control dynamically adjusts input signals in real-time based on the system's instantaneous state, ensuring effective chaos regulation with minimal external intervention. Feedback control plays a vital role in stabilizing the system, preventing extreme outcomes such as prey extinction or uncontrolled predator population growth. This approach is essential for effective ecosystem management and species preservation. Moreover, it offers a quantitative basis for informed decision-making, such as determining optimal predator release rates in biological pest control initiatives. Here, we employ a state feedback control strategy [45,46] to stabilize chaotic trajectories around an unstable fixed point in the proposed predator-prey system. The controlled dynamics are achieved by introducing a feedback control term σ_n into the prey component of system (2.2), yielding the modified equations:

$$\begin{aligned} x_{n+1} &= x_n + \delta\left[rx_n\left(1-\frac{x_n}{k}\right)\frac{1}{1+py_n} - \frac{(1-m)x_ny_n}{\beta+(1-m)x_n}\right] + \sigma_n(\mathbf{m},\mathbf{b}),\\ y_{n+1} &= y_n + \delta y_n\left[-d + \frac{\eta(1-m)x_n}{\beta+(1-m)x_n}\right]. \end{aligned} \tag{6.8}$$

The control input σ_n is defined as:

$$\sigma_n = -m_1(x_n - x^*) - m_2(y_n - y^*), \tag{6.9}$$

where m_1 and m_2 are feedback gains, and (x^*, y^*) denotes the unstable fixed point of the uncontrolled system (2.2).

The Jacobian matrix of the original system (2.2) evaluated at (x^*, y^*) is given by:

$$J(x^*, y^*) = \begin{pmatrix} l_{11} & l_{12} \\ l_{21} & l_{22} \end{pmatrix},$$

where the entries are:

$$l_{11} = \frac{\delta r(k-2x^*)}{kpy^*+k} + \frac{\beta\delta(m-1)y^*}{(\beta - mx^* + x^*)^2} + 1,$$
$$l_{12} = \delta\left(\frac{prx^*(x^*-k)}{k(py^*+1)^2} - \frac{x^* - mx^*}{\beta - mx^* + x^*}\right),$$
$$l_{21} = -\frac{\beta\delta\eta(m-1)y^*}{(\beta - mx^* + x^*)^2},$$
$$l_{22} = -d\delta + \frac{\delta\eta(m-1)x^*}{(m-1)x^* - \beta} + 1.$$

Under the influence of the control force σ_n, the controlled system's Jacobian becomes:

$$J_c(x^*, y^*) = \begin{pmatrix} l_{11} - m_1 & l_{12} - m_2 \\ l_{21} & l_{22} \end{pmatrix}. \tag{6.10}$$

The characteristic polynomial associated with $J_c(x^*, y^*)$ is derived in terms of the trace and determinant as:

$$\nu^2 - (l_{11} + l_{22} - m_1)\nu + [l_{22}(l_{11} - m_1) - l_{21}(l_{12} - m_2)] = 0. \tag{6.11}$$

This formulation allows for systematic stabilization by appropriately selecting the feedback gains, m_1 and m_2 to ensure the eigenvalues of J_c lie within the unit circle, thereby suppressing chaotic oscillations.

Let ν_1 and ν_2 denote the eigenvalues of the controlled system (6.10). From the characteristic polynomial (6.11), we derive the following relations:

$$\nu_1 + \nu_2 = l_{11} + l_{22} - m_1, \tag{6.12}$$

$$\nu_1\nu_2 = l_{22}(l_{11} - m_1) - l_{21}(l_{12} - m_2). \tag{6.13}$$

The stability boundary conditions are determined by setting $\nu_1\nu_2 = 1$ and $\nu_1 = \pm 1$. These constraints ensure that the eigenvalues lie within the unit circle, guaranteeing asymptotic stability.

Stability boundaries:

1) $\nu_1\nu_2 = 1$:

$$l_1 : l_{22}m_1 - l_{21}m_2 = l_{11}l_{22} - l_{12}l_{21} - 1.$$

2) $\nu_1 = 1$:

$$l_2 : (1 - l_{22})m_1 + l_{21}m_2 = l_{11} + l_{22} - 1 - l_{11}l_{22} + l_{12}l_{21}.$$

3) $\nu_1 = -1$:

$$l_3 : (1 + l_{22})m_1 - l_{21}m_2 = l_{11} + l_{22} + 1 + l_{11}l_{22} - l_{12}l_{21}.$$

The intersection of these three lines forms a bounded triangular region in the m_1m_2-plane, within which the controlled system exhibits stable dynamics. Any feedback gains (m_1, m_2) selected from this region stabilize the otherwise unstable fixed point.

Numerical validation: For the specific parameter set under consideration, the stability boundaries reduce to:

$$l_1 : m_1 - 0.545937m_2 = 0,$$
$$l_2 : 0.545937m_2 + 0.352571 = 0,$$
$$l_3 : 2m_1 - 0.545937m_2 - 3.64743 = 0.$$

The feasible stability region, depicted in Figure 7, illustrates the admissible range of feedback gains that ensure stabilization. Numerical simulations confirm the efficacy of the proposed control strategy in suppressing chaotic oscillations, as demonstrated in the accompanying figure.

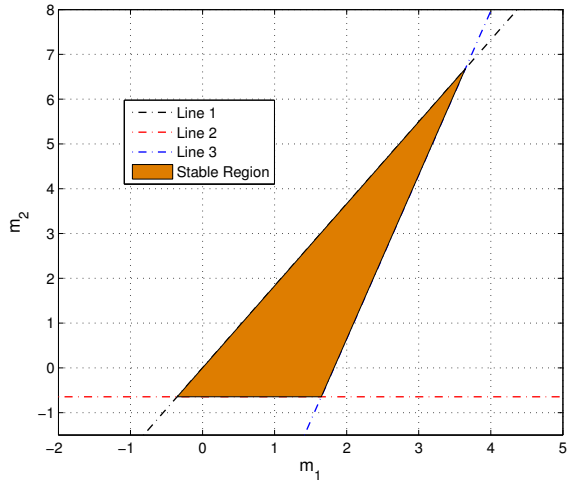

Figure 7. Stability region in the m_1m_2-plane, derived from the eigenvalue constraints.

7. Conclusions

The fear effect refers to the indirect influence predators exert on prey populations, where the mere presence or perceived threat alters prey behavior, physiology, or spatial distribution, even in the absence of direct predation. Understanding this ecological mechanism is crucial for effective conservation practices, pest management strategies, and maintaining ecosystem balance. This study investigates a discrete-time Rosenzweig-MacArthur predator-prey model incorporating prey fear effects and refuge strategies, which play a crucial role in shaping population dynamics. We conduct a local stability and bifurcation analysis, emphasizing Neimark-Sacker and period-doubling bifurcations to identify instability thresholds and transitions to chaotic regimes. To regulate these complex dynamics and maintain ecological equilibrium, we implement OGY and state feedback control, effectively managing bifurcations across a broad range of parameter values. Numerical simulations confirm our theoretical predictions, highlighting the model's ability to capture intricate predator-prey interactions.

Our results demonstrate that changes in the fear effect parameter can trigger bifurcations, identifying it as a critical factor in the stabilization or destabilization of the predator-prey system. From a biological standpoint, a moderate level of fear appears advantageous for both species, supporting previous studies on the influence of fear in predator-prey interactions. Providing refuge for prey improves their chances of survival, but can unintentionally jeopardize the persistence of predators. When combined, these

two ecological elements can lead to oscillations, recurring cycles, or even chaotic fluctuations in population dynamics. The observed stability of the positive fixed point underscores the complex long-term dynamics involved, emphasizing the substantial role that fear plays in shaping both prey and predator populations.

Author contributions

Md. Jasim Uddin: Methodology, computations, software, analysis, validation, supervision, writing-original draft, review and editing; Md. Mutakabbir Khan: Methodology, computations, analysis, validation, writing-original draft; Ibraheem M. Alsulami: Investigation, software, writing-original draft, review and editing; Amer Alsulami: Investigation, validation, writing-original draft. All authors have read and approved the final version of the manuscript for publication.

Use of Generative-AI tools declaration

The authors declare they has not used Artificial Intelligence (AI) tools in the creation of this article.

Acknowledgements

The authors extend their appreciation to Umm Al-Qura University, Saudi Arabia for funding this research work through grant number: 25UQU4340243GSSR03.

Funding

This research work was funded by Umm Al-Qura University, Saudi Arabia under grant number: 25UQU4340243GSSR03.

Conflicts of interest

The authors declare that they have no conflicts of interest.

References

1. H. I. Freedman, *Deterministic mathematical models in population ecology*, New York: Marcel Dekker, Inc., 1980. https://doi.org/10.2307/2530090
2. P. H. Leslie, J. C. Gower, The properties of a stochastic model for the predator-prey type of interaction between two species, *Biometrika*, **47** (1960), 219–234. https://doi.org/10.2307/2333294
3. M. Kot, *Elements of mathematical ecology*, Cambridge: Cambridge University Press, 2001. https://doi.org/10.1017/cbo9780511608520
4. A. Wikan, Ø. Kristensen, Prey-predator interactions in two and three species population models, *Discrete Dyn. Nat. Soc.*, **2019** (2019), 9543139. https://doi.org/10.1155/2019/9543139
5. S. L. Yuan, Y. L. Song, Bifurcation and stability analysis for a delayed Leslie–Gower predator-prey system, *IMA J. Appl. Math.*, **74** (2009), 574–603. https://doi.org/10.1093/imamat/hxp013

6. A. P. Maiti, B. Dubey, J. Tushar, A delayed prey-predator model with Crowley–Martin-type functional response including prey refuge, *Math. Method. Appl. Sci.*, **40** (2017), 5792–5809. https://doi.org/10.1002/mma.4429
7. S. Gakkhar, A. Singh, Complex dynamics in a prey-predator system with multiple delays, *Commun. Nonlinear Sci.*, **17** (2012), 914–929. https://doi.org/10.1016/j.cnsns.2011.05.047
8. S. Gakkhar, A. Singh, B. P. Singh, Effects of delay and seasonality on toxin producing phytoplankton-zooplankton system, *Int. J. Biomath.*, **5** (2012), 1250047. https://doi.org/10.1142/s1793524511001891
9. S. Kumar, H. Kharbanda, Chaotic behavior of predator-prey model with group defense and non-linear harvesting in prey, *Chaos Soliton. Fract.*, **119** (2019), 19–28. https://doi.org/10.1016/j.chaos.2018.12.011
10. M. Haragus, G. Iooss, *Local bifurcations, center manifolds, and normal forms in infinite-dimensional dynamical systems*, London: Springer, 2011. https://doi.org/10.1007/978-0-85729-112-7
11. A. Hastings, T. Powell, Chaos in a three-species food chain, *Ecology*, **72** (1991), 896–903. https://doi.org/10.2307/1940591
12. W. Liu, Y. P. Qin, C. L. Shi, D. D. Guo, Dynamic evolution of spontaneous combustion of coal in longwall gobs during mining-stopped period, *Process Saf. Environ.*, **132** (2019), 11–21. https://doi.org/10.1016/j.psep.2019.09.027
13. M. M. Zhao, J. C. Ji, Dynamic analysis of wind turbine gearbox components, *Energies*, **9** (2016), 110. https://doi.org/10.3390/en9020110
14. R. Ahmed, M. Rafaqat, I. Siddique, M. A. Arefin, Complex dynamics and chaos control of a discrete-time predator-prey model, *Discrete Dyn. Nat. Soc.*, **2023** (2023), 8873611. https://doi.org/10.1155/2023/8873611
15. A. E. Matouk, Chaos and bifurcations in a discretized fractional model of quasi-periodic plasma perturbations, *Int. J. Nonlin. Sci. Num.*, **23** (2022), 1109–1127. https://doi.org/10.1515/ijnsns-2020-0101
16. A. A. Elsadany, A. E. Matouk, Dynamical behaviors of fractional-order Lotka–Volterra predator-prey model and its discretization, *J. Appl. Math. Comput.*, **49** (2015), 269–283. https://doi.org/10.1007/s12190-014-0838-6
17. R. Ahmed, Complex dynamics of a fractional-order predator-prey interaction with harvesting, *Open J. Discret. Appl. Math.*, **3** (2020), 24–32. https://doi.org/10.30538/psrp-odam2020.0040
18. M. J. Uddin, C. N. Podder, Fractional order prey-predator model incorporating immigration on prey: complexity analysis and its control, *Int. J. Biomath.*, **17** (2024), 2350051. https://doi.org/10.1142/s1793524523500511
19. J. L. Xiao, The complex dynamics of sharing platform competition game, *Discrete Dyn. Nat. Soc.*, **2021** (2021), 2022179. https://doi.org/10.1155/2021/2022179
20. A. Al-Khedhairi, A. E. Matouk, S. S. Askar, Bifurcations and chaos in a novel discrete economic system, *Adv. Mech. Eng.*, **11** (2019), 1–15. https://doi.org/10.1177/1687814019841818

21. R. B. de la Parra, M. Marvá, E. Sánchez, L. Sanz, Discrete models of disease and competition, *Discrete Dyn. Nat. Soc.*, **2017** (2017), 5310837. https://doi.org/10.1155/2017/5310837
22. D. Mukherjee, Role of fear in predator-prey system with intraspecific competition, *Math. Comput. Simulat.*, **177** (2020), 263–275. https://doi.org/10.1016/j.matcom.2020.04.025
23. Y. X. Ma, R. Z. Yang, Bifurcation analysis in a modified leslie-gower with nonlocal competition and beddington-deangelis functional response, *J. Appl. Anal. Comput.*, **15** (2025), 2152–2184. https://doi.org/10.11948/20240415
24. F. Y. Zhu, R. Z. Yang, Bifurcation in a modified Leslie-Gower model with nonlocal competition and fear effect, *Discrete Cont. Dyn.-B*, **30** (2025), 2865–2893. https://doi.org/10.3934/dcdsb.2024195
25. E. González-Olivares, R. Ramos-Jiliberto, Dynamic consequences of prey refuges in a simple model system: more prey, fewer predators and enhanced stability, *Ecol. Model.*, **166** (2003), 135–146. https://doi.org/10.1016/s0304-3800(03)00131-5
26. T. K. Kar, Stability analysis of a prey-predator model incorporating a prey refuge, *Commun. Nonlinear Sci.*, **10** (2005), 681–691. https://doi.org/10.1016/j.cnsns.2003.08.006
27. S. M. S. Rana, M. J. Uddin, Dynamics and control of a discrete predator-prey model with prey refuge: Holling type I functional response, *Math. Probl. Eng.*, **2023** (2023), 5537632. https://doi.org/10.1155/2023/5537632
28. J. P. Tripathi, S. Abbas, M. Thakur, Dynamical analysis of a prey-predator model with Beddington–DeAngelis type function response incorporating a prey refuge, *Nonlinear Dyn.*, **80** (2015), 177–196. https://doi.org/10.1007/s11071-014-1859-2
29. H. Zhang, F. Tian, P. Harvim, P. Georgescu, Effects of size refuge specificity on a predator-prey model, *Biosystems*, **152** (2017), 11–23. https://doi.org/10.1016/j.biosystems.2016.12.001
30. Q. Yue, Dynamics of a modified Leslie–Gower predator-prey model with Holling-type II schemes and a prey refuge, *SpringerPlus*, **5** (2016), 461. https://doi.org/10.1186/s40064-016-2087-7
31. S. Sarwardi, P. K. Mandal, S. Ray, Dynamical behaviour of a two-predator model with prey refuge, *J. Biol. Phys.*, **39** (2013), 701–722. https://doi.org/10.1007/s10867-013-9327-7
32. N. Boccara, *Modeling complex systems*, 2 Eds., New York: Springer, 2010. https://doi.org/10.1007/978-1-4419-6562-2
33. M. W. Conkey, A. Beltrán, G. A. Clark, J. G. Echegaray, M. G. Guenther, J. Hahn, et al., The identification of prehistoric hunter-gatherer aggregation sites: the case of Altamira, *Curr. Anthropol.*, **21** (1980), 609–630. https://doi.org/10.1086/202540
34. M. L. Rosenzweig, R. H. MacArthur, Graphical representation and stability conditions of predator-prey interactions, *Am. Nat.*, **97** (1963), 209–223. https://doi.org/10.1086/282272
35. H. S. Zhang, Y. L. Cai, S. M. Fu, W. M. Wang, Impact of the fear effect in a prey-predator model incorporating a prey refuge, *Appl. Math. Comput.*, **356** (2019), 328–337. https://doi.org/10.1016/j.amc.2019.03.034
36. K. Sarkar, S. Khajanchi, Impact of fear effect on the growth of prey in a predator-prey interaction model, *Ecol. Complex.*, **42** (2020), 100826. https://doi.org/10.1016/j.ecocom.2020.100826
37. P. H. Leslie, A stochastic model for studying the properties of certain biological systems by numerical methods, *Biometrika*, **45** (1958), 16–31. https://doi.org/10.1093/biomet/45.1-2.16

38. X. Y. Wang, L. Zanette, X. F. Zou, Modelling the fear effect in predator-prey interactions, *J. Math. Biol.*, **73** (2016), 1179–1204. https://doi.org/10.1007/s00285-016-0989-1

39. M. Javidi, N. Nyamoradi, Dynamic analysis of a fractional order prey–predator interaction with harvesting, *Appl. Math. Model.*, **37** (2013), 8946–8956. https://doi.org/10.1016/j.apm.2013.04.024

40. Y. A. Kuznetsov, H. G. E. Meijer, Numerical normal forms for codim 2 bifurcations of fixed points with at most two critical eigenvalues, *SIAM J. Sci. Comput.*, **26** (2005), 1932–1954. https://doi.org/10.1137/030601508

41. M. J. Uddin, S. M. S. Rana, S. Işık, F. Kangalgil, On the qualitative study of a discrete fractional order prey-predator model with the effects of harvesting on predator population, *Chaos Soliton. Fract.*, **175** (2023), 113932. https://doi.org/10.1016/j.chaos.2023.113932

42. S. Lynch, *Dynamical systems with applications using mathematica*, 2 Eds., Cham: Birkhäuser, 2007. https://doi.org/10.1007/978-3-319-61485-4

43. E. Ott, C. Grebogi, J. A. Yorke, Controlling chaos, *Phys. Rev. Lett.*, **64** (1990), 1196. https://doi.org/10.1103/physrevlett.64.1196

44. M. J. Uddin, S. M. S. Rana, Qualitative analysis of the discretization of a continuous fractional order prey-predator model with the effects of harvesting and immigration in the population, *Complexity*, **2024** (2024), 8855142. https://doi.org/10.1155/2024/8855142

45. N. Li, H. Q. Yuan, H. Y. Sun, Q. L. Zhang, An impulsive multi-delayed feedback control method for stabilizing discrete chaotic systems, *Nonlinear Dyn.*, **73** (2013), 1187–1199. https://doi.org/10.1007/s11071-012-0434-y

46. K. Pyragas, Delayed feedback control of chaos, *Phil. Trans. R. Soc. A*, **364** (2006), 2309–2334. https://doi.org/10.1098/rsta.2006.1827

AIMS Press